A novel surface modification technique for forming porous polymer monoliths in poly(dimethylsiloxane)

Jeffrey M. Burke and Elisabeth Smela[a)]
Mechanical Engineering Department, University of Maryland, College Park, Maryland 20742, USA

(Received 23 October 2011; accepted 17 February 2012; published online 9 March 2012)

A new method of surface modification is described for enabling the *in situ* formation of homogenous porous polymer monoliths (PPMs) within poly(dimethylsiloxane) (PDMS) microfluidic channels that uses 365 nm UV illumination for polymerization. Porous polymer monolith formation in PDMS can be challenging because PDMS readily absorbs the monomers and solvents, changing the final monolith morphology, and because PDMS absorbs oxygen, which inhibits free-radical polymerization. The new approach is based on sequentially absorbing a non-hydrogen-abstracting photoinitiator and the monomers methyl methacrylate and ethylene diacrylate within the walls of the microchannel, and then polymerizing the surface treatment polymer within the PDMS, entangled with it but not covalently bound. Four different monolith compositions were tested, all of which yielded monoliths that were securely anchored and could withstand pressures exceeding the bonding strength of PDMS (40 psi) without dislodging. One was a recipe that was optimized to give a larger average pore size, required for low back pressure. This monolith was used to concentrate and subsequently mechanical lyse B lymphocytes.
 [http://dx.doi.org/10.1063/1.3693589]

I. INTRODUCTION

Microfluidic-based assays provide several key advantages over traditional bench-top techniques, including reduced regent consumption, ability to do parallel processing, and decreased analysis time. These devices can, however, become complicated, incorporating multiple unit operations such as separation, concentration, lysis, mixing, and detection. Achieving the desired fluid flow requires careful consideration of the microfluidic chip layout, valving, reagent addition, waste removal, and balancing of fluidic resistances. Thus, a system that combines two or more operations is advantageous, as it simplifies device design. To this end, we examined the use of a porous polymer monolith (PPM) formed within a poly(dimethylsiloxane) (PDMS) microfluidic device for cell concentration and subsequent lysis.

PPMs were first developed as an alternative approach to traditional packed beds in chromatographic columns.[1–4] In recent years, monoliths have been adopted by lab-on-a-chip devices because they can be polymerized *in situ* and functionalized using a variety of chemistries; monoliths have been used in a wide range of microfluidic applications, including chromatography,[5–9] solid phase extraction,[10–12] electrospray emitters,[13,14] and electroosmotic pumps.[15,16]

Despite the utility of monoliths and the widespread use of PDMS, there have been few reports integrating the two. This is likely due to difficulty in achieving homogeneous monoliths: PDMS is highly permeable to oxygen, which quenches free radical polymerization.[13] Furthermore, most of the monomers and porogenic solvents used to form the monoliths are readily absorbed into the PDMS.[17,18] It is, therefore, necessary to first modify the PDMS surface. Surface modification also provides functional groups that crosslink with the monolith to anchor it

[a)]Author to whom correspondence should be addressed. Electronic mail: smela@eng.umd.edu. Tel.: 301-405-5265. Fax: 301-314-9477.

in place so that gaps do not form at the walls and so that the monolith does not dislodge under applied pressure.

Various approaches for modifying the surface of PDMS have been investigated in order to control, among other things, surface charge, hydrophobicity, and functionalization.[19] For preparing PDMS for monolith polymerization, two approaches have been employed. The first is a silanization reaction commonly used for monolith production in glass devices.[12,20] Since PDMS does not have active silanol groups, it must first be oxidized, accomplished using either ultraviolet (UV) irradiation[21,22] or NaOH.[23] Although not reported in the monolith literature, O_2 plasma can also be used to oxidize PDMS.[24] Thereafter, the PDMS surface is silanized using an alkoxysilane terminated with a reactive species, such as a vinyl group,[20] that crosslinks with the monolith during polymerization.

The second approach to modification is via photografting, first shown to be an effective method for binding monoliths to cyclic olefin copolymers[25] and since adapted to other substrates, including PDMS.[13,17,26] Photografting involves the formation of radicals on the surface that serve as initiation sites for polymerization. The radicals are formed using a hydrogen-abstracting photoinitiator,[27–30] such as benzophenone. Typically, a two-step process has been used in which the benzophenone is pre-absorbed into the substrate followed by the introduction of the monomer[31,32] and irradiation using 254 nm UV light. The monomer reacts locally with the radicals on the channel surface, forming a thin modification layer with polymerizable vinyl moieties that can be crosslinked to the PPM.[25]

Given the popularity of SU-8 (MicroChem Corp., Newton, MA) and other i-line (365 nm) sensitive photoresists for MEMS applications,[33] it would be beneficial to have a procedure for forming a monolith in PDMS using 365 nm irradiation to take advantage of photolithography equipment already available to most research groups. Therefore, in this fabrication paper, we present an alternative method for channel modification (Fig. 1(a)). This approach initiates polymerization *within* the PDMS matrix. The photoinitiator is pre-absorbed into the PDMS, followed by the introduction into the channel of the modification solution, which is also absorbed. Upon irradiation with UV light (365 nm), polymerization proceeds within the PDMS. The resulting surface modification polymer is not covalently bound to the PDMS, but is instead entangled within it. The monolith is then polymerized within the channel (Fig. 1(b)). We show that the new surface layer firmly anchors the monolith within the microchannel. To illustrate the use of the monolith, B lymphocytes were trapped against a monolith frit. By controlling the flow rate, we were able to first concentrate the lymphocytes, and by subsequently increasing the flow rate, lyse them.

II. EXPERIMENTAL

A. Materials

PDMS (Sylgard 184) prepolymer and curing agent were obtained from Dow Corning (Midland, MI). Butyl methacrylate (BuMA), methyl methacrylate (MMA), ethylene dimethacrylate (EDMA), trimethylolpropane trimethacrylate (TMPTMA), ethylene diacrylate (EDA), benzophenone, 2,2-dimethoxy-2-phenyl-acetophenone (DMPAP), and sodium (meta)periodate were purchased from Sigma-Aldrich (St. Louis, MO). BuMA, MMA, EDMA, and TMPTMA were passed over an activated, basic alumina column (Brockmann I, 150 mesh) to remove the inhibitors. All others were used as purchased. Chloroform and methanol were obtained from Fischer Scientific (Pittsburg, PA) and acetone was obtained from J.T. Baker (Phillipsburg, NJ).

B. PDMS microchannel fabrication

PDMS microchannels 200 μm $\times$ 70 μm $\times$ 9.5 mm were fabricated using standard soft lithography.[34] A mixture of PDMS prepolymer solution and curing agent at a 10:1 ratio was cast over an SU-8 50 (MicroChem Corp., Newton, MA) master, cured at 50 °C for 2 h, and peeled off. Inlets and outlets were formed from 2.5 cm long, 0.89 mm I.D. silicone tubing.[35]

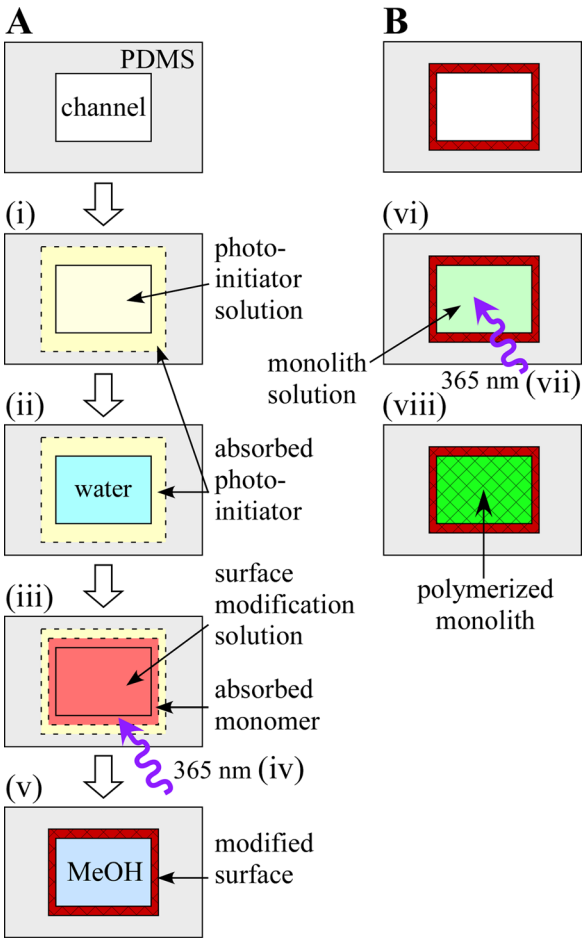

FIG. 1. (A) Schematic representation of the surface modification protocol. (i) Photoinitiator solution is introduced into the channel, and photoinitiator is absorbed into the PDMS microchannel walls. (ii) Depleted photoinitiator solution is flushed away. Steps (i) and (ii) are repeated. (iii) Surface modification solution is introduced into the channel and the monomers are absorbed into the channel walls. (iv) The channel is irradiated with 365 nm UV light and (v) flushed with methanol. (B) Schematic of monolith formation. (vi) Monolith solution is introduced into the channel. The device is (vii) irradiated with 365 nm UV light to polymerize the monolith and (viii) remaining monomers and porogens are rinsed away with methanol.

The PDMS substrate with the channels was irreversibly bonded to a second PDMS slab using O_2 plasma (8 s at 450 mTorr and 50 W).

C. PDMS surface modification

The surface of the PDMS microchannels was modified using the procedure described in Fig. 1(a). Briefly, the channels were flushed with 0.25 M DMPAP in chloroform for 1 min followed by flushing with water for 1 min. This process was performed twice to ensure that a substantial amount of DMPAP had been absorbed into the PDMS. The surface modification polymerization mixture was then pumped into the channels, the inlet and outlet were sealed, and the system was allowed to rest for 1 min to allow the monomers to diffuse into the PDMS. This mixture consisted of two monomers, 50% MMA and 50% EDA by weight. Black electrical tape was used as a photomask to define the location and length of the modification. The device was exposed to UV light (365 nm) using either a handheld 8 W light source (UVP, Upland, CA) or a higher power 100 W light source (UVP, Upland, CA) for 40 or 30 s, respectively. Following irradiation, the channel was flushed with methanol to remove the unreacted monomer.

D. Monolith formation

Monolith solutions (Table I) were sonicated for 10 min followed by purging with N_2 gas for 15 min. The monolith solution was introduced into the channel, the inlet and outlet were sealed, and the solution was irradiated through the photomask for 45 min using an 8 W hand-held UV lamp. Using a 100 W UV lamp, the irradiation time was reduced to 15 min, which is compatible with mask aligners found in most academic clean rooms. Following exposure, the channels were flushed with methanol to remove the porogen and any unreacted monomers and then stored in de-ionized (DI) water to ensure the stability of the monolith: if allowed to dry, the monoliths shrunk, cracking at the channel wall.[36]

E. Scanning electron microscopy

Images of the monoliths were taken with a scanning electron microscope (SEM) (Hitachi SU-70) at an acceleration voltage of 10 kV. SEM samples were prepared by cutting vertically through the monolith-filled PDMS channels. Gold was sputtered onto the samples prior to SEM imaging.

F. Monolith pressure test

Monolith pressure tests were conducted by pumping methanol through the monoliths using compressed N_2 gas. The pressure was increased at a rate of $\sim$5 psi/min until the there was either noticeable flow through the outlet or failure of the PDMS device.

G. Cell concentration and shear-induced mechanical lysis

B lymphocytes were obtained from Innovative Biosensors, Inc. (Rockville, MD). Initial cell concentrations were determined using a hemocytometer. Cells at a concentration of 3.25×10^5 cells/ml were injected into the PDMS device for 20 min at a flow rate of 2 μl/min using a syringe pump (New Era NE-1000). The cells were then washed with L-15 media for 20 min at 2 μL/min. To lyse the cells, the flow rate was increased to 5 μL/min.

III. RESULTS AND DISCUSSION

A. Surface modification

Prior to polymerization of the monolith, the surface of the PDMS microchannel must be modified to provide an anchoring layer for the covalent attachment of the monolith. Such modifications have also been reported to limit the absorption of the monolith monomers into the PDMS (Refs. 17 and 18) and to minimize the diffusion of oxygen into the channel.[13]

Without surface modification (Fig. 2(a1)), a gap formed between the monolith (recipe C, see below) and the channel wall (Fig. 2(a2)), presumably as a result of monolith shrinkage during polymerization. Under moderate pressures, the monolith plug can become dislodged from the desired location. Omitting the surface modification also resulted in radial heterogeneity:

TABLE I. Compositions of the four monolith solutions (in wt. %).

	Monomer	Crosslinker	Crosslinker	Porogen	Photoinitiator
Monolith	BuMA	EDMA	TMPTMA	Decanol	DMPAP
A[a]	23.8	15.8	—	60.0	0.4
B[b]	11.9	27.7	—	60.0	0.4
C[c]	14.9	—	24.7	60.0	0.4
D	10.4	24.3	—	65.0	0.3

[a]Adapted from Stachowiak *et al.*[25]
[b]Adapted from Mair *et al.*[51]
[c]Adapted from Liu *et al.*[10]

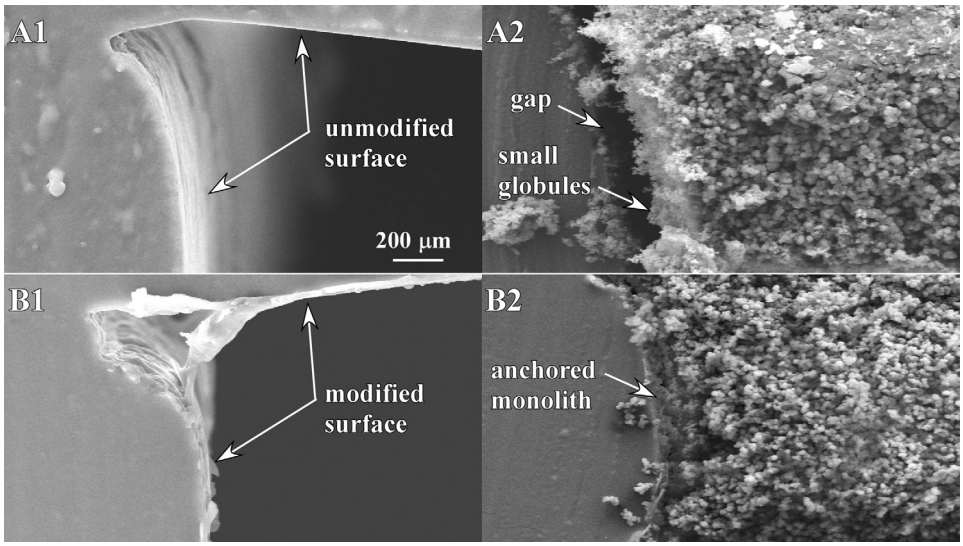

FIG. 2. SEM images showing the effects of surface modification of PDMS. (A1) Unmodified, empty channel. (A2) Monolith formed in an unmodified channel. (B1) Empty surface-modified channel. (B2) Monolith formed in a surface-modified channel.

near the wall, the monoliths consisted of small, densely packed globules, while at the center the globules were substantially larger. It is reasonable to suppose that the smaller globules were the result of slower reaction kinetics due to inhibition by oxygen in the PDMS.

When using the previously reported protocol for the surface modification of PDMS,[31] which had benzophenone as the photoinitiator, with a 365 nm UV light source, the monoliths formed but were unattached to the channels walls. Though other groups have shown photografting using benzophenone and 365 nm light,[37,38] it was reported that the procedure had to be done at least four times in order to provide sufficient surface modification for anchoring the monolith.[26] The reason for this is that photografting with benzophenone is optimal with light in the range of 200–300 nm; outside of that, the rate of polymerization decreases and the grafting efficiency approaches zero.[29]

DMPAP has a higher absorption at 365 nm than benzophenone and it enhances radical polymerization because it contains additional electron-donating groups that can undergo a secondary excitation, resulting in four, rather than the typical two, radical groups.[39] However, unlike benzophenone, DMPAP is not a hydrogen-abstracting photoinitiator, and so one would not expect the reaction to proceed from radical formation on the channel wall. In fact, simply substituting DMPAP for benzophenone in the photografting protocol resulted in polymerization of the surface modification solution only at the middle of the channel. Therefore, it was necessary to devise a new approach for surface modification of PDMS using 365 nm irradiation.

In our new procedure (Fig. 1), which is similar to the sol gel modification procedure developed by Roman *et al.*,[40] the surface modifying monomers were absorbed into the PDMS matrix and then polymerized there. Technically, this new procedure is not photografting because the surface modification layer is not covalently bonded to the PDMS. Instead, this technique has been shown to result in the modification layer becoming intertwined within the polymer chains of the PDMS.[32] Surface modification began with flushing the channels with 0.25 M DMPAP in chloroform. Chloroform extensively swells PDMS,[41] and so allows absorption of the photoinitiator. Chloroform has a high permeability in PDMS (~160 times that of oxygen)[42] so essentially all the chloroform would have evaporated from the PDMS prior to use of the device. No problems with PDMS bonding or monolith formation due to the presence of the chloroform were observed. However, it should be noted that small channels (less than ~10 μm in the smallest dimension) can become fully blocked as the PDMS swells. Although not explored in this fabrication paper, if minute amounts of chloroform are problematic for

certain applications, it is likely that acetone could be used instead of chloroform because it also swells PDMS (Ref. 41) and has been shown in other publications to help pre-absorb photoinitiators into PDMS.[31]

Following absorption of the DMPAP into the PDMS, the channels were flushed with water and filled with the surface modification polymerization mixture, consisting of two monomers, 50% MMA, and 50% EDA. Since the DMPAP is pre-absorbed into the PDMS, upon exposure to UV light (365 nm), polymerization of the surface modification monomers initiates only within the PDMS. As the reaction proceeds, the surface modification monomers crosslink and branch, extending into the microchannel.[32] This modification layer has an abundance of polymerizable vinyl groups, which later become incorporated with, and ultimately anchor, the monolith.[25] We found an optimal irradiation time of 40 s for an 8 W light source where surface modification monomer polymerization only occurred near the channel wall and within the PDMS (Fig. 2(b1)). This is consistent with work reported by Wang *et al.*[32] in which they showed that pre-absorption of the photo-initiator followed by absorption of acrylic acid and exposure to UV light yielded an interpenetrating polymer network that extended 50 μm into the PDMS substrate and 150 nm above the surface. Since they were using benzophenone, a hydrogen-abstracting photoinitiator, they proposed two mechanisms by which the polymer network was formed: (1) benzophenone free-radicals abstract hydrogen atoms from the methyl side groups of the PDMS, leading to covalent attachment of the surface modification layer to the PDMS and (2) benzophenone free-radicals directly initiating polymerization of the acrylic acid within the PDMS. In our case, the surface modification solution is not covalently bound since we are not using a hydrogen-abstracting photoinitiator.

Instead, only polymerization of the surface modification monomers within PDMS occurs, yet monoliths subsequently formed in the treated channels using this method appeared in the SEM images to be anchored, with no gap. The radial heterogeneity of the monolith also improved, showing a range of globule sizes that was consistent across the channel (Fig. 2(b2)). This is likely because of decreased O_2 permeation into the channel due to the surface modification.

B. Monolith formation

To test the anchoring ability of the surface modification layer and to check for the presence of gaps between the monoliths and the channel walls, the pressures required to flow liquid through them were determined. The compositions of four monolith solutions that were tested are given in Table I. Three were adapted from previously published recipes (monoliths A, B, and C), and the fourth was a new recipe optimized for use in our PDMS microchannels (monolith D). Detailed characterization of the monoliths was not an aim of this fabrication paper, since that has been previously reported.[9,43–45] Instead, the aims were to test the efficacy of the surface modification method and to determine the conditions required to produce a monolith in PDMS that is homogenous not only radially, but also axially, along the channel length. Because PDMS microfluidic devices, unlike poly(methyl methacrylate) (PMMA) or glass devices, have a maximum operating pressure of ~40 psig due to failure of PDMS-PDMS bonding, monoliths with a larger average pore size were desired. It had previously been shown that the pore size can be controlled by the type and concentration of the monomer, crosslinker, porogen, and initiator.[9,43,46–50]

Fig. 3 shows SEM and optical microscope images of the four monoliths. All exhibited the interconnected, microglobule network that was expected. However, monolith A was discontinuous, with sections containing voids (Fig. 3(a)). Monolith homogeneity is critical for most applications. Consistent pore size is required for uniform flow patterns, and uniform surface chemistry and charge are needed for good chromatographic separations, binding, and electroosmotic flow. Inhomogeneity is caused by, among other things, concentration gradients and oxygen. It has also been suggested by several groups[10,11] that flow within the microfluidic channel during polymerization gives rise to such inhomogeneous structures. Following their suggestions, the device was left to rest undisturbed for 10 min before exposure to minimize pressure gradients, but there was no noticeable improvement. We suspect that the reaction kinetics of this mixture were too slow, likely due to the presence

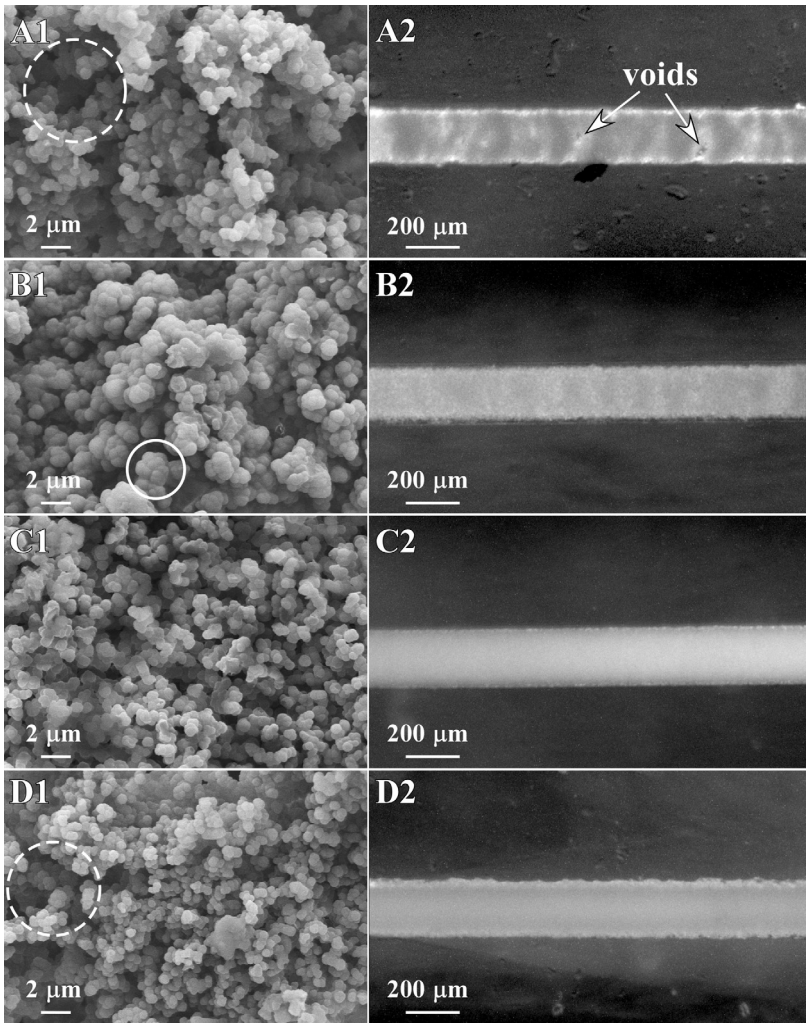

FIG. 3. (A1) SEM image of monolith A with a macropore indicated within the dashed circle. (A2) Overhead stereomicroscope image of monolith A. (B) Monolith B with an example of fused globules at the center of the white circle in B1. (C) Monolith C. (D) Monolith D, with the dashed circle indicating a macropore.

of oxygen, to produce a homogeneous monolith within PDMS. Monolith A was, therefore, not evaluated further.

Monolith B had a higher crosslinker concentration than monolith A. This increased the reaction kinetics[51] and, as expected, the monolith had improved heterogeneity (Fig. 3(b)). However, increasing the crosslinker concentration also leads to monoliths with smaller pores.[49] A comparison of the SEM images shows a fundamental difference between monoliths A and B. Although the globule size was roughly the same, the pores were smaller for monolith B because the increased crosslinker concentration caused the globules to fuse during polymerization.[51]

To test the pressure required to pump liquid through the monolith, monoliths of various lengths (0.7 mm–4 mm) were formed. Compressed nitrogen gas was used to pump methanol through the monoliths. These pressure tests were conducted immediately following polymerization when the devices were flushed with methanol to remove the porogen and the unreacted monomers. Because of the high viscosity of the monomer solution, the pressure required to push liquid through the monolith is higher than it is under normal operation, and, as a result, device failure is more likely to occur.

Monolith B required 12.4 psi per mm of monolith length to pump liquid through. Failure of the PDMS devices occurred routinely at 40 psi. This limited the length of monolith B to

$\sim$3 mm. All devices longer than 3 mm failed due to the high pressures. This high pressure requirement could limit the applications for monolith B.

The recipe for monolith C was chosen because it uses a different crosslinker, TMPTMA instead of EDMA. TMPTMA has three methacrylate groups from which the reaction can proceed, compared with two for EDMA.[10] Using TMPTMA increased the reaction kinetics and yielded monoliths that were homogeneous but that had small pores (Fig. 3(c)). During pressure testing, none of the C monoliths, regardless of length, exhibited flow before device failure. The use of this recipe with PDMS is, therefore, not recommended.

In an attempt to develop a monolith with lower backpressure that would be better suited for applications in PDMS, we explored the effect of varying the concentration of the porogenic solvent, keeping everything else constant. Increasing the relative amount of the porogen yields a monolith without changing the overall composition or surface chemistry of the monolith. Monolith B was chosen as the base case, and the concentration of decanol was varied from 60%-80% in 5% increments. At concentrations of 75% and 80%, inhomogeneous monoliths were formed. At the intermediate concentrations of 65% and 70%, the monoliths had lower backpressures, with those formed with 65% porogen (Monolith D) showing better homogeneity.

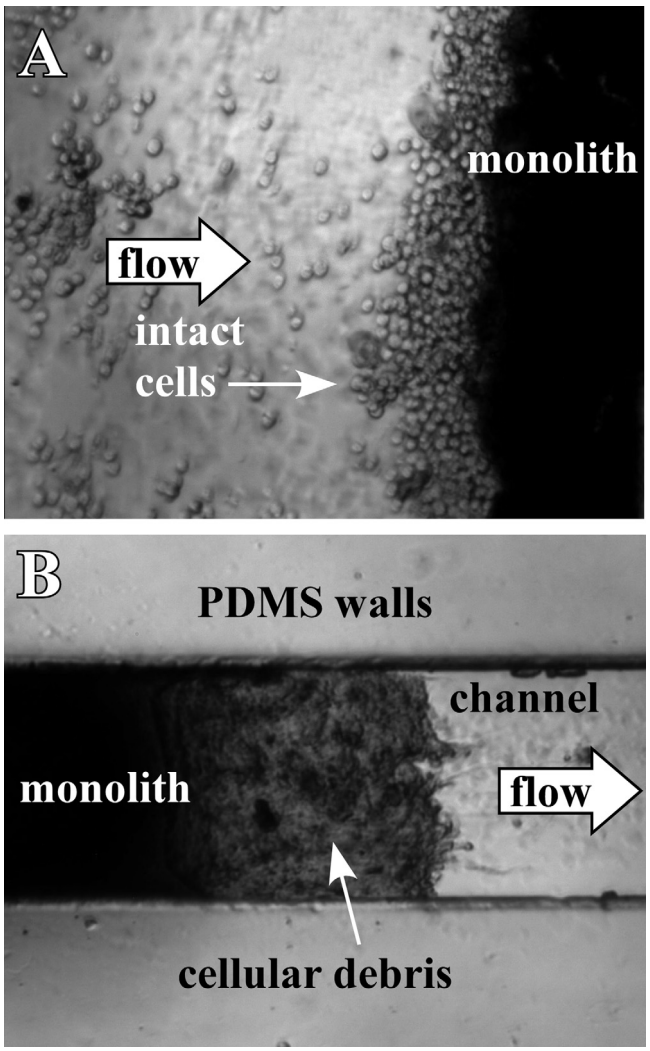

FIG. 4. (A) Optical microscope image of live B lymphocytes trapped against the inlet side of a monolith (monolith D). (B) At flow rates above 4 μl/min, increased shear caused the lymphocytes to lyse, and cellular debris appeared at the outlet of the monolith.

The axial homogeneity of monolith D was comparable to that of monoliths B and C (Fig. 3(d)). However, monolith D had larger macropores (Fig. 3(d)), which had flow at only 6.8 psi/mm of monolith, a 45% reduction in back pressure compared to monolith B. As a result, monoliths of up to 6 mm could be used without device failure.

IV. LYMPHOCYTE CONCENTRATION AND SHEAR-INDUCED MECHANICAL LYSIS

To illustrate a potential application of monoliths formed in PDMS using this new surface modification technique, concentration of cells followed by shear-induced mechanical lysis was demonstrated. Monolith D was formed within a PDMS microchip, and B lymphocytes at an initial concentration of 3.25×10^5 cells/ml were injected into the device at a flow rate of 2 μl/min. Fig. 4(a) shows the cells concentrating against the monolith. They could be mechanically lysed by simply increasing the flow rate. This forced the cells to enter the small pores of the monolith, leading to increased shear stress on the cell membrane and mechanical lysis.[52] To determine the flow rate required for lysis, the flow was increased every 10 min by 0.5 μl/min. At a flow rate of 5 μl/min, cellular debris became noticeable at the outlet side of the monolith (Fig. 4(b)). Further increasing the flow rate resulted in increased cell lysis. In our study, clogging of the monolith did not occur. These results show that the monolith remained anchored under experimental pressures, while allowing usable flows (>5 μl/min) without failure of the PDMS device.

An inherent advantage of using a monolith to lyse cells is that following lysis and liberation of the genomic DNA the monolith can be used to capture and concentrate the nucleic acids. This has been illustrated in the literature through the incorporation of silica particles, which bind the DNA, into the monolith.[53–55] For this application, having a monolith with a lower backpressure, which allows the use of longer monoliths, will ensure sufficient nucleic acid binding capacity.

V. CONCLUSIONS

In this fabrication paper, we have introduced a novel method for surface modification that involves intertwining a surface modification polymer within the PDMS at the channel walls. With this surface modification, monoliths could be anchored at pressures exceeding the bonding strength of the PDMS structures. Monoliths have various applications, and this surface modification method provides users with an alternative approach which uses 365 nm UV light, compared to 250 nm. To illustrate a potential application of this surface modification method, B lymphocytes were first concentrated and then lysed using the monolith.

ACKNOWLEDGMENTS

We acknowledge the support of the Maryland NanoCenter and its FabLab and NispLab. This material is based upon work supported by the National Science Foundation under Grant Nos. II50515873 and II50813773. We would like to thank Dr. Mark Kujawski for his assistance with SEM imaging. We would also like to thank Innovative Biosensors, Inc. (Rockville, MD) for providing the B lymphocytes used in this work.

[1]S. Hjerten, J. L. Liao, and R. Zhang, J. Chromatogr. **473**, 273 (1989).
[2]F. Svec and J. M. J. Frechet, Anal. Chem. **64**, 820 (1992).
[3]T. B. Tennikova, M. Bleha, F. Svec, T. V. Almazova, and B. G. Belenkii, J. Chromatogr. **555**, 97 (1991).
[4]Q. C. Wang, F. Svec, and J. M. J. Frechet, Anal. Chem. **65**, 2243 (1993).
[5]K. Faure, M. Albert, V. Dugas, G. Cretier, R. Ferrigno, P. Morin, and J. L. Rocca, Electrophoresis **29**, 4948 (2008).
[6]J. Krenkova, A. Gargano, N. A. Lacher, J. M. Schneiderheinze, and F. Svec, J. Chromatogr. A **1216**, 6824 (2009).
[7]D. Lee, F. Svec, and J. M. J. Frechet, J. Chromatogr. A **1051**, 53 (2004).
[8]C. Yu, F. Svec, and J. M. J. Frechet, Electrophoresis **21**, 120 (2000).
[9]C. Yu, M. C. Xu, F. Svec, and J. M. J. Frechet, J. Polym. Sci., Part A: Polym. Chem. **40**, 755 (2002).
[10]J. K. Liu, C. F. Chen, C. W. Tsao, C. C. Chang, C. C. Chu, and D. L. Devoe, Anal. Chem. **81**, 2545 (2009).

[11]J. D. Ramsey and G. E. Collins, Anal. Chem. **77**, 6664 (2005).
[12]C. Yu, M. H. Davey, F. Svec, and J. M. J. Frechet, Anal. Chem. **73**, 5088 (2001).
[13]M. F. Bedair and R. D. Oleschuk, Anal. Chem. **78**, 1130 (2006).
[14]P. Wang, Z. Chen, and H. C. Chang, Electrophoresis **27**, 3964 (2006).
[15]J. A. Tripp, F. Svec, J. M. J. Frechet, S. L. Zeng, J. C. Mikkelsen, and J. G. Santiago, Sens. Actuators B **99**, 66 (2004).
[16]P. Wang, Z. L. Chen, and H. C. Chang, Sens. Actuators B **113**, 500 (2006).
[17]K. Faure, M. Bias, O. Yassine, N. Delaunay, G. Cretier, M. Albert, and J. L. Rocca, Electrophoresis **28**, 1668 (2007).
[18]S. W. Hu, X. Q. Ren, M. Bachman, C. E. Sims, G. P. Li, and N. Allbritton, Anal. Chem. **74**, 4117 (2002).
[19]J. W. Zhou, A. V. Ellis, and N. H. Voelcker, Electrophoresis **31**, 2 (2010).
[20]C. Ericson, J. L. Liao, K. Nakazato, and S. Hjerten, J. Chromatogr. A **767**, 33 (1997).
[21]H. L. Zeng, H. F. Li, and J. M. Lin, Anal. Chim. Acta **551**, 1 (2005).
[22]H. L. Zeng, H. F. Li, X. Wang, and J. M. Lin, Talanta **69**, 226 (2006).
[23]Y. Xu, W. P. Zhang, P. Zeng, and Q. Cao, Sensors **9**, 3437 (2009).
[24]M. K. Chaudhury, and G. M. Whitesides, Langmuir **7**, 1013 (1991).
[25]T. B. Stachowiak, T. Rohr, E. F. Hilder, D. S. Peterson, M. Q. Yi, F. Svec, and J. M. J. Frechet, Electrophoresis **24**, 3689 (2003).
[26]Q.-S. Kang, Y. Li, J.-Q. Xu, L.-J. Su, Y.-T. Li, and W.-H. Huang, Electrophoresis **31**, 3028 (2010).
[27]B. Ranby, W. T. Yang, and O. Tretinnikov, Nucl. Instrum. Methods Phys. Res. B **151**, 301 (1999).
[28]W. T. Yang and B. Ranby, J. Appl. Polym. Sci. **62**, 533 (1996).
[29]W. T. Yang and B. Ranby, Polym. Bull. **37**, 89 (1996).
[30]F. W. Deeg, J. Pinsl, and C. Brauchle, J. Phys. Chem. **90**, 5715 (1986).
[31]S. W. Hu, X. Q. Ren, M. Bachman, C. E. Sims, G. P. Li, and N. L. Allbritton, Anal. Chem. **76**, 1865 (2004).
[32]Y. L. Wang, H. H. Lai, M. Bachman, C. E. Sims, G. P. Li, and N. L. Allbritton, Anal. Chem. **77**, 7539 (2005).
[33]W. Wang and S. A. Soper, *Bio-MEMS: Technologies and Applications* (CRC, Boca Raton, 2007).
[34]D. C. Duffy, J. C. McDonald, O. J. A. Schueller, and G. M. Whitesides, Anal. Chem. **70**, 4974 (1998).
[35]M. E. Piyasena, R. Newby, T. J. Miller, B. Shapiro, and E. Smela, Sens. Actuators B **141**, 263 (2009).
[36]B. H. Gu, Z. Y. Chen, C. D. Thulin, and M. L. Lee, Anal. Chem. **78**, 3509 (2006).
[37]M. H. Schneider, Y. Tran, and P. Tabeling, Langmuir **27**, 1232–1240 (2011).
[38]M. H. Schneider, H. Willaime, Y. Tran, F. Rezgui, and P. Tabeling, Anal. Chem. **82**, 8848 (2010).
[39]J. P. Fisher, D. Dean, P. S. Engel, and A. G. Mikos, Annu. Rev. Mater. Res. **31**, 171 (2001).
[40]G. T. Roman, T. Hlaus, K. J. Bass, T. G. Seelhammer, and C. T. Culbertson, Anal. Chem. **77**, 1414 (2005).
[41]J. N. Lee, C. Park, and G. M. Whitesides, Anal. Chem. **75**, 6544 (2003).
[42]I. Blume, E. Smit, M. Wessling, and C. A. Smolders, Makromol. Chem., Macromol. Symp. **45**, 237 (1991).
[43]S. Eeltink, J. M. Herrero-Martinez, G. P. Rozing, P. J. Schoenmakers, and W. T. Kok, Anal. Chem. **77**, 7342 (2005).
[44]J. J. Ou, G. T. T. Gibson, and R. D. Oleschuk, J. Chromatogr. A **1217**, 3628 (2010).
[45]E. C. Peters, F. Svec, J. M. J. Frechet, C. Viklund, and K. Irgum, Macromolecules **32**, 6377 (1999).
[46]S. Eeltink, E. F. Hilder, L. Geiser, F. Svec, J. M. J. Frechet, G. P. Rozing, P. J. Schoenmakers, and W. T. Kok, J. Sep. Sci. **30**, 407 (2007).
[47]S. Eeltink and F. Svec, Electrophoresis **28**, 137 (2007).
[48]F. Svec, J. Chromatogr. A **1217**, 902 (2010).
[49]F. Svec and J. M. J. Frechet, Ind. Eng. Chem. Res. **38**, 34 (1999).
[50]C. Viklund, F. Svec, J. M. J. Frechet, and K. Irgum, Chem. Mater. **8**, 744 (1996).
[51]D. A. Mair, T. R. Schwei, T. S. Dinio, F. Svec, and J. M. J. Frechet, Lab Chip **9**, 877 (2009).
[52]M. D. Kulinski, M. Mahalanabis, S. Gillers, J. Y. Zhang, S. Singh, and C. M. Klapperich, Biomed. Microdevices **11**, 671 (2009).
[53]A. Bhattacharyya and C. A. Klapperich, Sens. Actuators B **129**, 693 (2008).
[54]A. Chatterjee, P. L. Mirer, E. Z. Santamaria, C. Klapperich, A. Sharon, and A. F. Sauer-Budge, Anal. Chem. **82**, 4344 (2010).
[55]M. Mahalanabis, H. Al-Muayad, M. D. Kulinski, D. Altman, and C. M. Klapperich, Lab Chip **9**, 2811 (2009).